Characterization of Ultrasonic and Radar Reflector Types in Concrete by Phase Evaluation of the Signal and the Reconstructed Image

Klaus MAYER, Karl-Jörg LANGENBERG, University of Kassel, Department of Electrical Engineering and Computer Science, Electromagnetic Field Theory, Kassel, Germany
Martin KRAUSE, Christiane MAIERHOFER, Boris MILMANN, Christoph KOHL, Federal Institute for Materials Research and Testing, Berlin, Germany

Abstract. Echo methods combined with imaging evaluation allow for investigation of the inner structure of concrete members. Ultrasonic echo and impulse radar data are analysed with reconstruction calculation procedures like 3D-SAFT (Synthetic Aperture Focusing Technique) and 3D-FT-SAFT (Fourier-Transform SAFT). From the representations of the 3D-data sets (B-scans and C-scans) the location of reinforcement bars, tendon-ducts, air voids and honeycombing can be deduced.

In order to localise ungrouted areas (air inclusions) in tendon ducts or to decide whether a reflector measured with radar is metallic (reinforcement) or air-like (void), up to now the interpretation of the results is based on the intensity of the reflection. This criterion is non unique in most cases, because the intensity of the backscattered waves is also influenced by the coupling conditions of the probes or by local variations of the concrete properties.

A new approach is to take the phase information into account. The phase information contained in the impulse-like data or in the complex type reconstructed image can help to decide whether the wave pulses pass from concrete to a denser material (e.g. steel) or to a less dense material (e.g. air), even layer thicknesses can be characterized. Since the evaluation of the data usually does not consider single A-scans but reconstructed data, the phase analysis has to be integrated in the reconstruction procedure.

In order to investigate and improve the method, a specimen with planar reflectors was used containing four steel-plates of different thickness partly covered with polystyrene (symbolising air-like reflection) and the wave propagation was simulated by the FIT (Finite Integration Technique) method.

Introduction

Caused by the strong heterogeneous structure of the media the wave propagation in concrete is very hard to be described mathematically. Nevertheless relevant methods exist for the detection of defects or of defective embedded structures. Imaging methods applied to measured data gained at surfaces allow the multidimensional display of the scattered intensities to find the position and size of the scattering inhomogeneity. A classification in respect of the criticality of an indication is not given automatically by the imaging algorithm, but requires more exact investigations of each indication by the inspector and an exact analysis of the circumstances which lead to the indication. Up to now the relevant evaluation criterion is the amplitude dynamic of the indication [1] [2] [3].

In concrete the wave propagation is distorted by the stochastic arrangement of aggregates with different acoustic properties and pores. The methods which are based on the analysis of the time delay require that the wave fronts stay together and this is only the case, if wavelengths are selected which are larger than the aggregates. This fact leads to a limitation of the resolution of the imaging algorithm, which then is in the range of the wavelength. In concrete with an incident shear wave of 55 kHz and a typical average wave speed of c_s = 2600 m/s the wavelength is 47 mm. Therefore it is evident that objects like tendon ducts can be detected but the content cannot be imaged exactly.

Imaging algorithms like SAFT (Synthetic Aperture Focusing Technique) calculate on the assumption of further approximations a “band limited” object function of the scatterer. “Band limited” however means, that the reconstruction is resolution limited und oscillating. This oscillation is disturbing because a slice out of the 2D or 3D reconstruction would show these oscillations and a unique peak detection would not be possible - at least by visual inspection of the images. This is the reason why during SAFT processing an envelope is calculated which suppresses the oscillations similar to a peak rectification with sample and hold. The processing methods differ for different implementations of the SAFT algorithm. Even though SAFT as a mathematically based algorithm is reconstructing an object function which is real and which contains the reflection coefficient at the scattering geometry, the band limitation and the envelope detection are the most prominent limiting factors which are to be considered during the interpretation procedure [4][5][6].

The second factor is based on the fact, that SAFT-like methods are mathematically derived on an assumption which is not fulfilled in the actual application: SAFT does not take multiple reflections into account. I.e. parts of the signal which are caused by multiple reflections are not focused to those positions where they occur physically but lead to artefacts – ghost images – degrading the correct image. Those artefacts are recognisable if the multiple reflections are separable in the time range. But this is not the case if the multiple echoes are smeared together and are combined to one single indication.

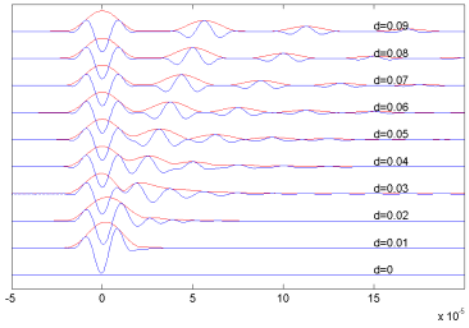

Figure 1: Reflection of a RC2 shear wave pulse of 50kHz at a steel plate in concrete with variation of the thickness (normalized amplitude)

Figure 1 demonstrates the signal behaviour of a scattering process at a steel plate in concrete. The variation of the thickness of the plate demonstrates how the signal of the back wall approaches more and more to the signal of the front surface until both pulses combine to one single pulse. In addition, the envelope of the signal allows the separation of the pulses at 50 kHz until a plate thickness of about 20 mm is reached. After that the signals combine themselves to one signal. Observing the detailed pulse form for this (simulated) experiment an effect attracts attention which can be used for the characterization of the scattering process: by the delayed superposition of single pulses up to a delay of zero the pulse form is changing and delivers additional information about the scattering processes. As the change of the pulse form is not caused by geometrical effects which are covered by the SAFT process, it is transported into the SAFT image and can be used there, too, to gain additional information about the scattering process.

The detailed analysis of the pulse behaviour is rather complex and can only be made plausible here. But it is important to differentiate between effects caused by the wave propagation from the transducer to the scatterer and back again and by the scattering process itself.

Basic Feature

Definition and Determination of the Phase of a Pulse-like Signal

Considering the reflection coefficient $R(\omega,d)$ for the particle displacement of an elastic shear wave for normal incidence on a plate with the thickness d in a full space

$$R(\omega,d)=\frac{\frac{z_1-z_2}{z_1+z_2}-\frac{z_3-z_2}{z_3+z_2}e^{2jk_2d}}{1-\frac{z_1-z_2}{z_1+z_2}\frac{z_3-z_2}{z_3+z_2}e^{2jk_2d}}, \tag{1}$$

with the acoustic wave impedances z_i of the different layers, and k_2, the wave number within the plate, two particularities attract attention.

Firstly: the reflection coefficient is frequency dependent and secondly: it is complex. To get the reflected signal, $R(\omega,d)$ has to be multiplied by the spectrum of the pulse or a convolution of the inverse Fourier transform by the incoming pulse itself has do be performed. Using a raised cosine pulse with 2 cycles (RC2) with the centre frequency of 50 kHz yields the signals of Figure 1. The complex reflection coefficient describes the complete signal behaviour – the chain of pulses as well as the superposition to a single pulse. The frequency dependent reflection coefficient leads to the separation of the incident pulse into many multiple reflections for a thick plate as well as to the deformation of the single pulse for a thin plate. In Figure 2 the magnitude and the phase of $R(\omega,d)$ are displayed for a plate thickness of 20 mm.

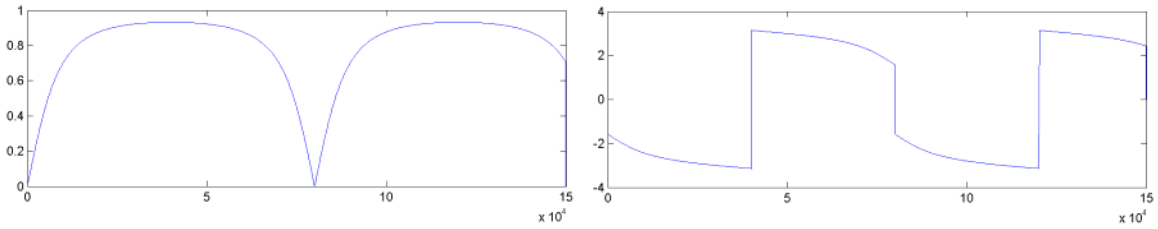

Figure 2 : Magnitude and phase of $R(\omega,d)$ at a thickness of 20 mm (frequency axis in Hz)

The phase dependency on the thickness at the centre frequency is displayed in Figure 3. Indeed the phase at the centre frequency is a measure for the thickness of the plate and characterizes the scattering process even if it is not possible to separate the multiple reflections.

The phase of the complex reflection coefficient in eq. (1) is referred to the coordinate system, i.e. to that point on the time axis, when the incident wave reaches the front of the plate. Relative to the symmetry axis of the RC2 impulse it is that time when the peak of the pulse reaches the front of the plate. For the practical measurement the position of the front of the scatterer and the time when the wave reaches the scatterer are not known but should be determined by the measurement itself. This means that the reference system for any scattering process has to be defined appropriately.

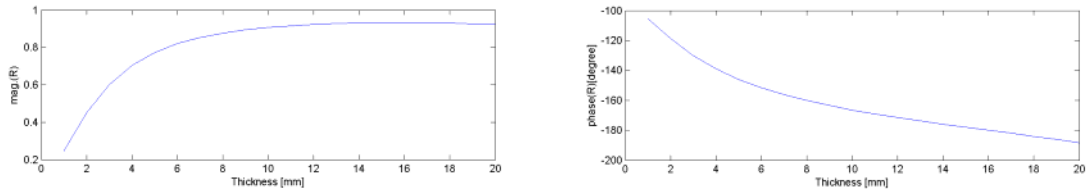

Figure 3: Dependency of amplitude and phase on the thickness of the plate at 50 kHz

For the following experiments as reference for the phase evaluation the maximum value of the envelope of the analytic signal was used. For measured data the calculation uses $s_e(t) = \sqrt{s(t)^2 + \mathrm{H}(s(t))^2}$, where H is the Hilbert transform of the signal $s(t)$. The FT-SAFT algorithm (SAFT calculated via Fourier Diffraction Slice Theorem) yields the envelope as the absolute value of the complex-valued reconstruction result. During a time domain SAFT processing the envelope can be achieved by calculating the absolute value of a complex SAFT calculation of the analytic signal which is the combination of the data as the real part and the Hilbert transform of the data as the imaginary part or as a not fully equivalent alternative by the envelope calculation of the reconstructed image into the depth direction.

As the phase of a pulse in the data the phase of the spectral component at the centre frequency f_0 within the interval $[t_0 - 1/f_0, t_0 + 1/f_0]$ is used. In the reconstructed image as the phase of a scattering indication at a depth z_0 the phase of the spectral component at the imaged wavelength λ_i within the interval $[z_0 - \lambda_i, z_0 + \lambda_i]$ is calculated.

As already mentioned the position of the maximum changes if the thickness of the plate is changing, whereas the reference of the phase in eq.(1) remains unchanged. Therefore, the theoretically calculated value for the phase cannot coincide with the value derived from the pulse itself by the calculation scheme above. Figure 4 compares the results for both calculations at the centre frequency. The difference is clearly visible and also the point, if the thickness of the plate is large enough, so that the estimation scheme is able to separate the pulses. If the thickness of the plate reaches the critical point the indicated phase jumps to the phase of the incident pulse which is 180° because the reflection coefficient at the transition of two plane simple media is real-valued.

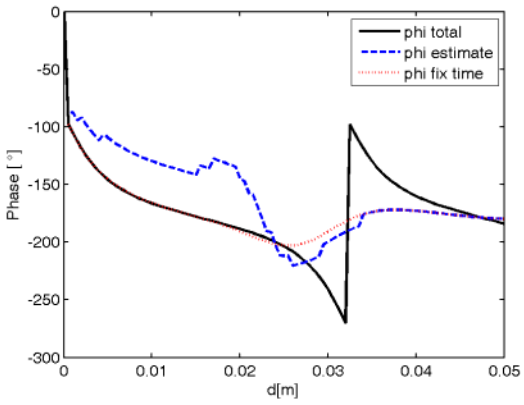

Figure 4: Comparison of the phase calculated from eq. (1) (solid line) with the phase from the phase estimation scheme (blue dashed line) and the phase estimated with a fixed reference time (red dashed line)

Visualisation of results

In the field of ultrasonic NDT the graphical display of scattered data and reconstructed images is done by grey or colour scaled intensity images with a non standardised colour table. For the display of the phase a combination of a grey and a colour table is appropriate. In ultrasonic B- or C- scans (slices along the beam axis respectively slices parallel to the surface) parts of the signal, which are below the detection level, are displayed in a grey scale and the detected pulses are coded according to an appropriate colour table, where the inten-

sity is additionally coded into the colour saturation. In case only black and white images can be used a hatched pattern coding is necessary. Figure 5 shows the phase detection applied to the signal of the plate with variation of the plate thickness into the y-direction.

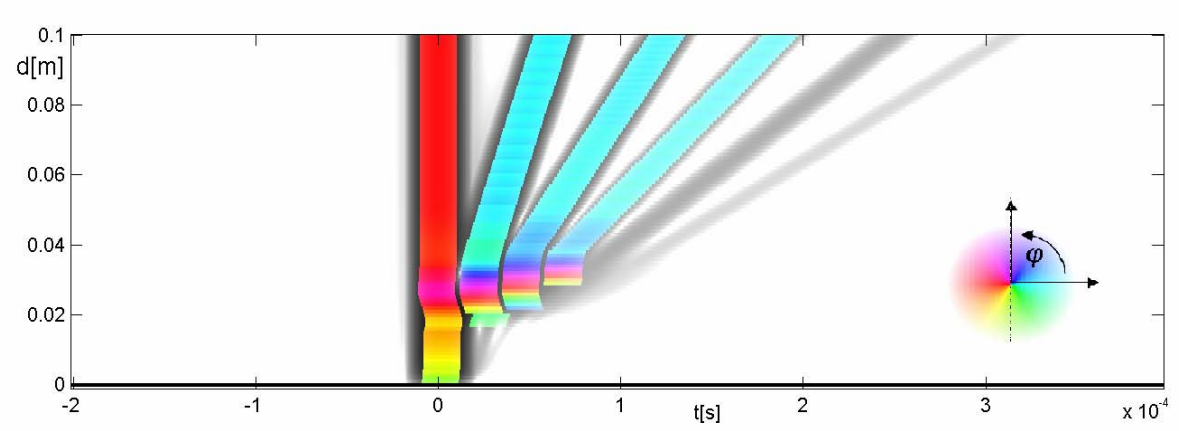

Figure 5: Phase detection with variation of the plate thickness *d* displayed along the detected pulses

Application Examples

As the problem of grouting defects of tendon ducts is of central importance in the area of NDT of concrete buildings - especially bridges of reinforced concrete are concerned – examples of this area have been selected to verify the capabilities of the method. With the aid of 2D- and 3D-EFIT (Elastodynamic Finite Integration Technique) [7][8] different typical examples have been simulated and evaluated. Figure 6 shows the wave propagation excited by a 40 mm pressure wave transducer at a frequency of 100 kHz. The wave has already reached the back wall of the tendon duct which is filled with steel wires, mortar and an air gap behind the front wall of the tendon duct. Figure 7 shows the 2D-FT-SAFT reconstruction of the simulated data together with the result of another simulation, where the air gap is behind the steel wires. The difference is clearly visible and the colour table shows a phase difference of about 160° for the indication of the front side of the tendon duct, which is enough to get a clear classification of the grouting defect.

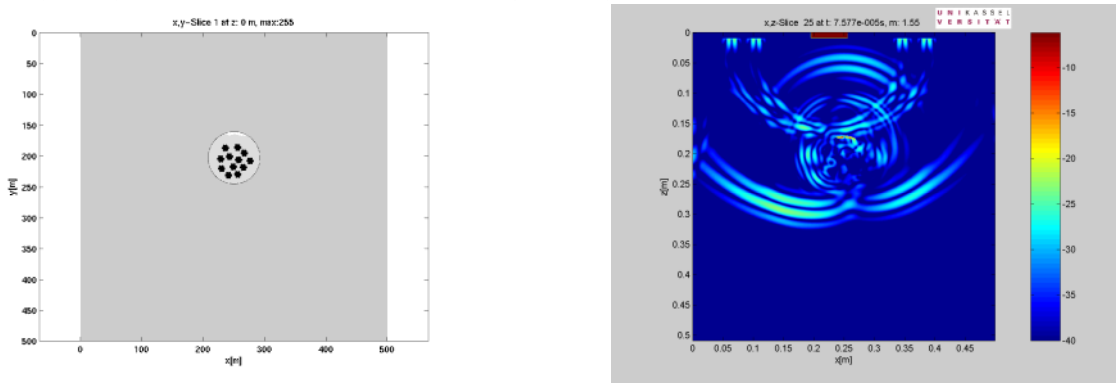

Figure 6: EFIT simulation of a 100 kHz pressure wave pulse in concrete. Left: modelled geometry, right: snapshot of the wave field (magnitude of the velocity vector)

In case the depth of the scatterer is known and the shape of the excitation signal is appropriate an alternative to the phase estimation method is to observe the real part of the instantaneous value of the reconstructed image. Small changes in the phase are clearly visible as changes of zero crossings of the oscillation and may be visualised by using sign-

dependent colouring. Figure 9 shows a C-scan of a 3D-SAFT image in the depth of the tendon duct and the defect is detected immediately.

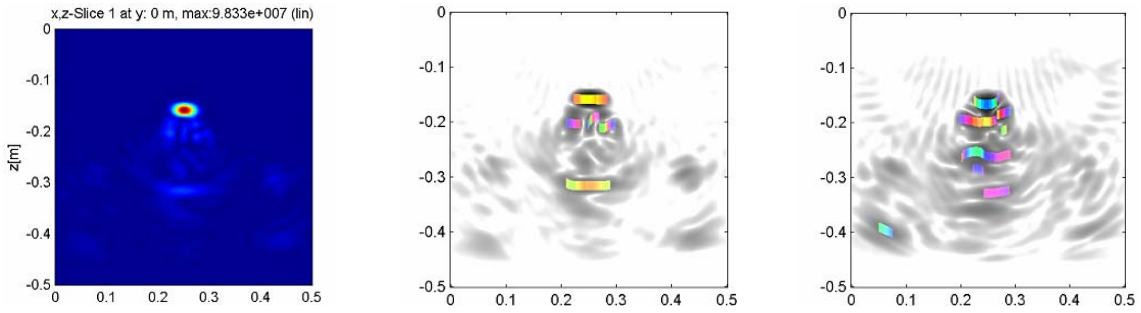

Figure 7: 2D-FT-SAFT reconstruction of the simulated data of Figure 6 together with a simulation with the air gap behind the steel wires

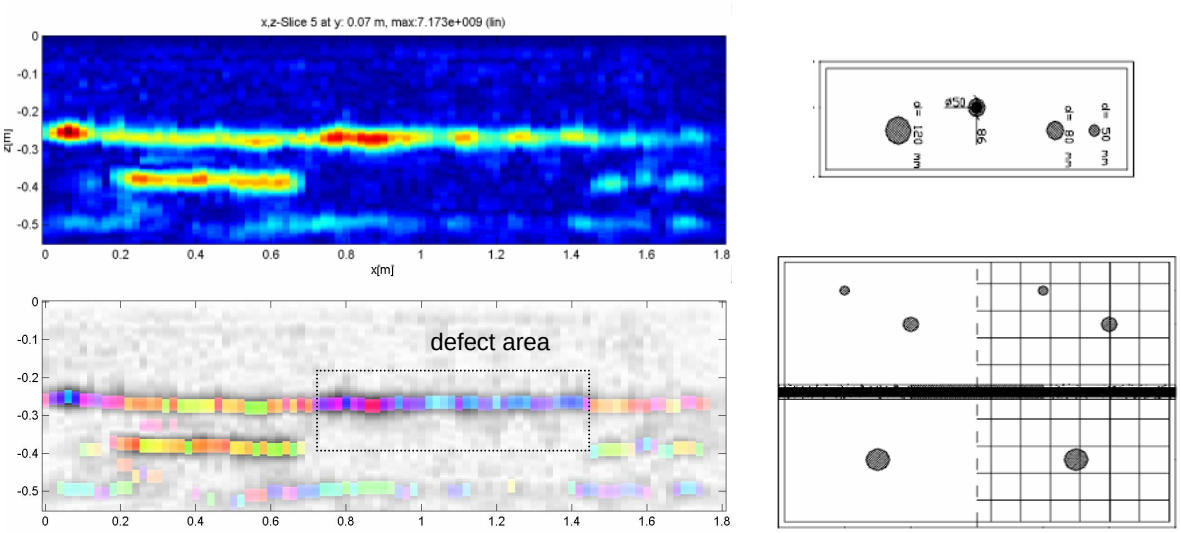

Figure 8: Amplitude and phase image of a 3D-FT-SAFT reconstruction of a concrete specimen with a synthetic grouting defect

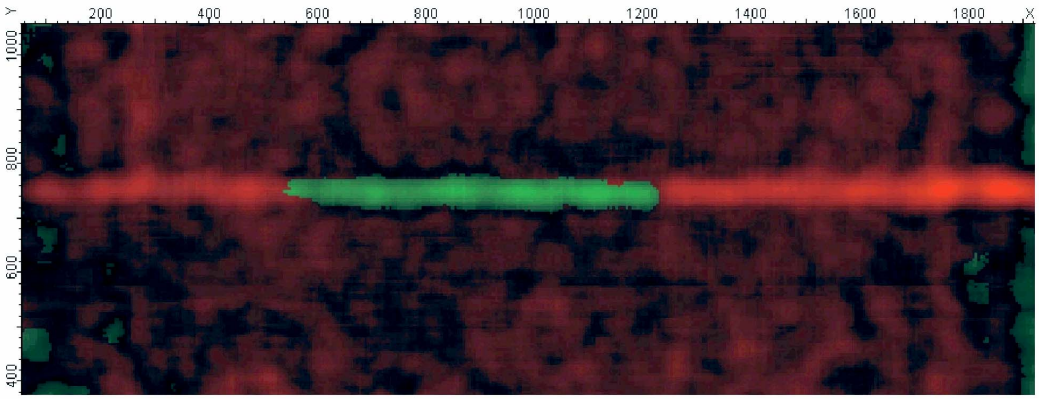

Figure 9: Display of the real part of the C-scan of a 3D-SAFT reconstruction with sign-dependent colour code

For an experimental verification the measurement at a concrete specimen containing a tendon duct with a synthetic grouting defect was evaluated. The measurement was performed with an A1220 shear wave transducer at 55 kHz. The tendon duct in the depth of 0.27 m was partially grouted in the indicated range. Additionally, an air gap behind the

steel strings in the range of 0.2 m to 0.6 m occurred accidentally. Figure 8 shows the 2D-magnitude and the phase image out of a 3D-FT-SAFT reconstruction and two drawings of the specimen which clearly indicates the performance of the method.

As a real live application the large area measurements at a concrete bridge in Vienna which was scanned with different ultrasonic and radar methods could be used. The 3D-FT-SAFT reconstruction of the six layers of tendon ducts with a diameter of 40 mm and filled with one tie rod with a diameter of 32 mm shows anomalies at different places which could be identified at least in the front layer as grouting defects. Test drillings confirmed those indications. Figure 10 shows the magnitude and the estimated phase of a layer (C-scan) out of the 3D-FT-SAFT reconstruction in the depth of the first layer of the tendon ducts together with a photography of the scene. It is interesting to see, that the phase indication shows anomalies even if the magnitude of the reconstruction gives only very small reflection amplitudes.

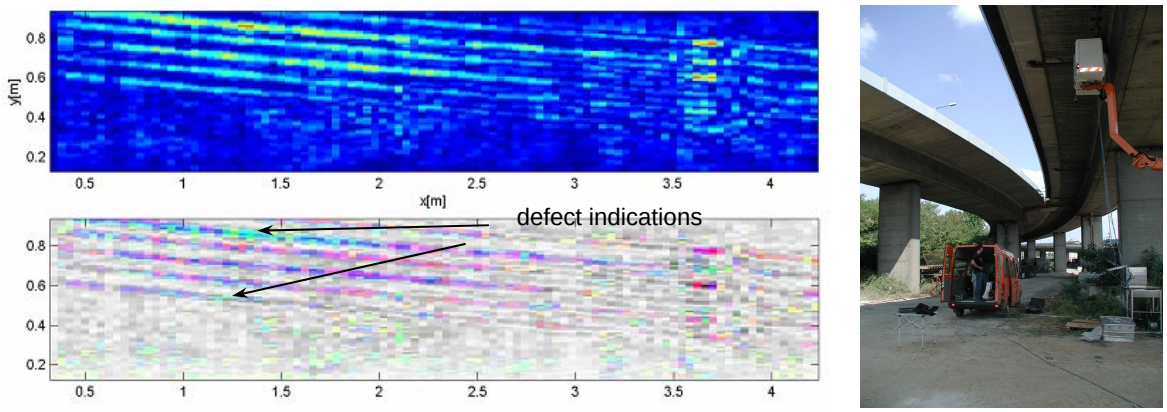

Figure 10: Amplitude and phase image of a 3D-FT-SAFT reconstruction gained at a real bridge building – C-scan in the depth of the first layer of tendon ducts

A complementary technique to localize tendon ducts and other structures in concrete is the application of pulse radar [9]. Because the mathematical treatment of the propagation of electromagnetic waves is related to the treatment of acoustic and elastic waves, similar algorithms can be used to focus the radar waves back to the scattering obstacles [5] [6]. Therefore the discussion of the phase above holds for electromagnetic waves, too. The selected example shows results of a concrete specimen designed to verify transition of concrete to steel and air. This specimen contains steel plates of different thicknesses and some planar polystyrene plates to simulate air. Figure 11 gives a short overview of this experiment and two orthogonal slices out of the 3D-FT-SAFT reconstruction with additional phase estimation. The scattering at polystyrene plates gives a phase of about -70° to -80° (green coloured) and the steel plates give an indication of about 70° to 90° (blue coloured).

Conclusion

Additionally observing the phase of signals and indications from imaging processes like SAFT or FT-SAFT gives a superior knowledge of the scattering process and can be successfully used for classification of many types of scattering problems in the field of NDT. The exact value of the phase depends on many circumstances and investigations of it will be given by the authors in the near future.

Acknowledgements

Support on basic research is gratefully acknowledged by Deutsche Forschungsgemeinschaft (DFG, German Research Council) via grant number FOR 384. Although not mentioned, many thanks to the people at BAM providing so many measurements and data to assist in solving such exciting problems. All support is gratefully acknowledged.

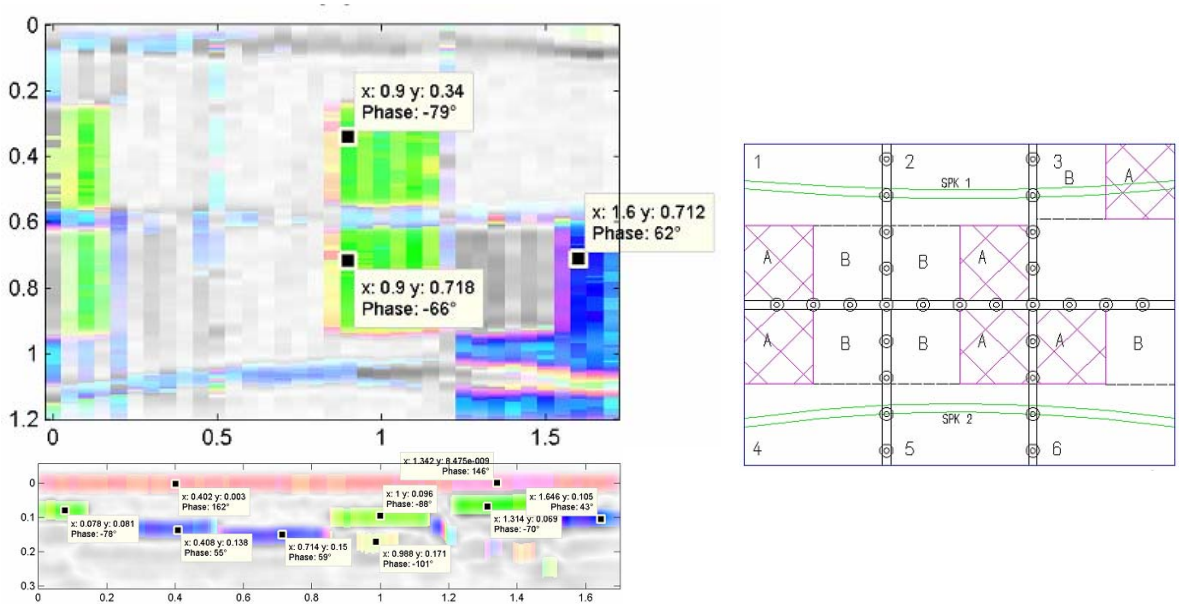

Figure 11: Phase analysis of a 3D-FT-SAFT reconstruction of a pulse radar experiment – (x, y)-C-scan (top-left), (x, z)-B-scan (bottom left) and top view drawing (right)

References

[1] M. Krause, F. Mielentz, B. Milmann, D. Streicher and W. Müller: Ultrasonic imaging of concrete elements: State of the art using 2D synthetic aperture. In: DGZfP (Ed.): International Symposium of Non-destructive Testing in Civil engineering (NDT-CE) in Berlin, Germany, September 16-19, 2003, Proceedings on BB 85-CD, V51, Berlin (2003);

[2] O. Kroggel, J. Scherzer and R. Jansohn: The Detectability Of Improper Filled Ducts With Ultrasound Re-flection Techniques. NDT.net – March 2002, Vol. 7 No. 03;

[3] M. Schickert, M. Krause and W. Müller: Ultrasonic Imaging of Concrete Elements using SAFT Reconstruction, Journal of Materials in Civil Engineering 15 (2003) 3, S. 235-246

[4] K. Mayer, R. Marklein, K.J. Langenberg and T. Kreutter: Three-dimensional imaging system based on the Fourier transform synthetic aperture technique. Ultrasonics 28 (1990) 241

[5] K.J. Langenberg, K. Mayer and R. Marklein: Nondestructive testing of concrete with electromagnetic and elastic waves: Modeling and imaging. Cement & Concrete Composites 28 (2006) 370

[6] K.J. Langenberg, M. Brandfaß, R. Hannemann, C. Hofmann, T. Kaczorowski, J. Kostka, R. Marklein, K. Mayer and A. Pitsch: Inverse scattering with acoustic, electromagnetic and elastic waves as applied in nondestructive evaluation. In: Wavefield Inversion. Ed.: A. Wirgin. Springer, Vienna 1999

[7] R. Marklein: EFIT simulations for Ultrasonic NDE. Proceedings of the ECNDT 2002 Conference, Barcelona, Spain, June 17-21, 2002.

[8] R. Marklein: The Finite Integration Technique as a general tool to compute acoustic, electromagnetic, elastodynamic and coupled wave fields. In: Review of Radio Science 1999–2002. Ed.: W.R. Stone. IEEE Press, Piscataway 2002

[9] Ch. Maierhofer: Nondestructive Evaluation of Concrete Infrastructure with Ground Penetrating Radar. In: Journal of Materials in Civil Engineering, Vol. 15, No. 3, May/June 2003, pp. 287-297